New precision determination of g_P and G_F: the MuXperiments at PSI

Bernhard Lauss

Physics Department, University of California,

366 LeConte Hall, Berkeley, CA 94720, USA

lauss@berkeley.edu

on behalf of the MuCAP [1] and MuLAN [2] collaborations

We discuss two precision experiments which will measure fundamental weak interaction parameters: MuLAN's goal is the measurement of the positive muon lifetime to 1 ppm, which will in turn determine the Fermi coupling constant G_F to 0.5 ppm precision. MuCAP is the first experiment which will unambiguously determine the induced pseudoscalar form factor of the proton, g_P. While contradictory experimental results for g_P are under discussion, firm theoretical calculations on the percent level within the framework of Chiral Perturbation Theory are now challenging the measurements. We will describe our experimental efforts and latest achievements.

1 Precision determination of G_F - the MuLAN experiment

We have seen impressive advances in our precise knowledge of many parameters defining the electroweak interaction within the Standard Model. However, the value of one of the most fundamental weak parameters, the Fermi coupling constant G_F, has not been improved in over two decades (see Fig.1). Usually G_F is determined via a measurement of the muon lifetime τ_μ

$$\frac{1}{\tau_\mu} = \frac{G_F^2 m_\mu^5}{192\pi^3} F\left(\frac{m_e^2}{m_\mu^2}\right)\left\{1 + \frac{3}{5}\frac{m_\mu^2}{M_W^2}\right\}\left(1 + \Delta_{QED}(\alpha_{m_\mu})\right) , \qquad (1)$$

with $F(x) = 1 - 8x - 12x^2 \ln x + 8x^3 - x^4$ [3]. The QED corrections within the Fermi Model, Δ_{QED}, are included in this definition.

Within the Standard Model one can derive the relation

$$G_F = \frac{\pi\alpha(0)}{\sqrt{2}M_W^2\left(1-\frac{M_W^2}{M_Z^2}\right)}(1+\Delta_r)\ , \tag{2}$$

with weak radiative corrections being summarized in Δ_r [4]. The calculated quantity Δ_r depends on the entire set of input parameters, e.g. M_Z, M_{Higgs}, m_{top}, α. Recently, these calculations were improved to the sub-ppm level by including numerically important QCD and electroweak higher-order terms up to 2-loop level. Therefore a precise comparison between theoretical and experimental values, e.g. for M_W (Eq. 2) is possible [4]. Consequently, G_F sets important constraints on the Standard Model and SUSY parameters. Furthermore, G_F sets the weak scale and is intimately connected to the vacuum expectation value of the Higgs field. The best possible experimental measurement of G_F at the present technological limit is therefore highly desirable, as the 18 ppm precision limit on the PDG average on τ_μ [5] is dominated by experimental counting statistics.

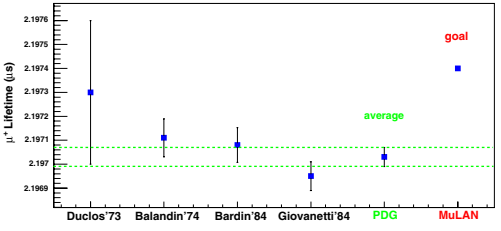

Figure 1: Progression of positive muon lifetime measurements [5]. The 1 ppm error goal of MuLAN is too small to be visible on this scale.

The MuLAN experiment (**Mu**on **L**ifetime **AN**alysis), intents to measure a total of 10^{12} μ^+ decays, in order to achieve a 1 ppm statistical error in the lifetime. Since the status report on the MuXprogram in [6] we have achieved substantial progress. A modification of the continuous high intensity muon beam line at the Paul Scherrer Institut was necessary to enable the collection of 10^{12} events within a reasonable time. We have built an electrostatic kicker which applies an artificial time structure to the DC beam in the πE3 area and found a kickable beam tune which provides up to 8 MHz of muons. Following a 5 μs muon collection period in the target, the kicker deflects the beam for 27 μs while muon decays are measured.

MuLAN is designed to minimize the systematic errors in several ways:

• **Muon polarization:** The beam muons are highly polarized, and the preferential emission of decay positrons in muon spin direction could cause a position- and time-dependent positron detection efficiency as polarized muons rotate in an external magnetic field. We are currently investigating two specific targets: i) Arnokrome-3 (Fig.2b) is a proprietary chromium-cobalt-iron alloy sheet, which, due to an internal field of a few Tesla, precesses muons very fast with respect to muon decay. Therefore polarization effects are negligible. ii) A solid sulfur target which maximizes the depolarization of the

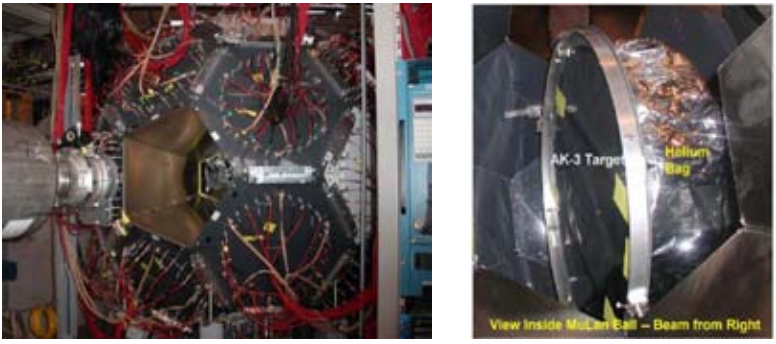

(a) (b)

Figure 2: The installed MuLAN setup:
a) View of the soccer ball detector. The visible hexagonal structures are made of six neighboring triangular scintillator pairs.
b) The Helium bag and the AK3 target mounted in the detector center.

beam muons. It is placed in a homogeneous 120 Gauss magnetic field which causes a fast visible muon rotation and allows us to fit the corresponding decay positron asymmetry. We are presently investigating samples of 10^{10} decay positrons from each target to select the optimal material choice. Additionally, a polarization-preserving silver target is being used for control purposes.
MuLAN's highly modular detector (Fig.2a) of 174 coincident scintillator tile pairs in "soccer ball" geometry allows us to compare opposite counters, thus strongly reducing precession effects in the count rate sum.

• **"Sneaky muons:"** A fast thin entrance muon counter (EMC) records beam muons and looks for muons sneaking in during the measurement interval. A magnet positioned behind the EMC precesses the tiny fraction of muons stopped in the detector materials, otherwise they too could cause small detection inefficiencies.

• **Off-target muon stopping:** Muon stops before the target are minimized by decreasing the materials in the muon path. Consequently we installed a helium bag (Fig.2b) and used very thin mylar windows and EMC materials.

• **Pile-up:** The high detector modularity and the fast scintillator response time reduce pile-up. Additional time resolution will be gained via new 500 MHz waveform digitizers (WFD) presently under construction, which will provide a double pulse resolution better than 4 ns. Final WFD implementation to all detector channels is planned for 2005.

The MuLAN detector (Fig.2a) was successfully commissioned in 2004 and yielded its first physics data. Fig.3 shows a 10 minute snapshot from our AK3 target data. We used multi-hit TDCs for detector readout. The muon accumulation time and the decay recording time are indicated. Our present analysis goal with this data is a 5 ppm precision determination of G_F. We intend to collect the full statistics in 2006.

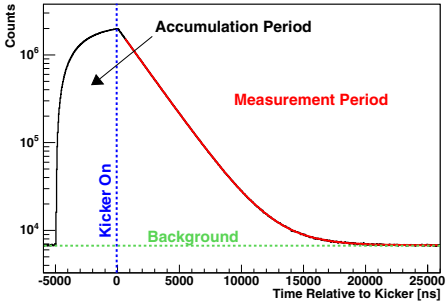

Figure 3: Lifetime spectrum (decay positron minus start of beam kick time) obtained in a single 10 minute run displaying accumulation and measurement period.

2 Precision determination of g_P - the MuCAP experiment

The $V-A$ description of weak interactions has been tested to a high precision. Processes involving structureless fermions, e.g. muon decay, show equal vector (V) and axial-vector (A) coupling. In β-decay as well as in nuclear muon capture on the proton $\mu^- + p \rightarrow \nu_\mu + n$, the axial coupling G_A is modified due to hadronic effects caused by the involved nucleon. Muon capture occurs at higher four-momentum transfer $q = -0.88 m_\mu^2$ than β-decay. Lorentz invariance constrains the corresponding weak current matrix elements to six independent terms,

$$V_\mu = G_V(q^2)\gamma_\mu - \frac{iG_M(q^2)}{2m_N}\sigma_{\mu\nu}q^\nu + \frac{G_S(q^2)}{m_\mu}q_\mu \quad (3)$$

$$A_\mu = G_A(q^2)\gamma_\mu\gamma_5 + \frac{G_P(q^2)}{m_\mu}\gamma_5 q_\mu + \frac{iG_T(q^2)}{2m_N}\sigma_{\mu\nu}q^\nu\gamma_5 \ , \quad (4)$$

with corresponding weak form factors G_i ($_i$ = scalar, pseudoscalar, vector, axial-vector, tensor, weak magnetism); mass of the nucleon m_N and muon m_μ. Because of G-symmetry G_S and G_T vanish [7]. Due to the momentum dependence, only G_A and G_V contribute in β-decay at very low q^2. Nuclear muon capture is the process most sensitive to G_P. Therefore, $G_P(-0.88 m_\mu^2)$ is dubbed induced pseudoscalar coupling constant g_P. While the values of G_V, G_A and G_M are established on the 10^{-3} to 10^{-4} level [5], the situation is totally different for the induced pseudoscalar g_P.

The theoretical view, historically based on PCAC and pion pole dominance, and recently strictly derived within chiral perturbation theory (χPT) [8], is remarkably precise:

$$G_P(q^2) = \frac{2m_\mu g_{\pi NN} F_\pi}{m_\pi^2 - q^2} - \frac{1}{3c^2\hbar^2}G_A(0)m_\mu m_N r_A^2 \ , \quad (5)$$

$$g_P = (8.74 \pm 0.23) - (0.48 \pm 0.02) = 8.23 \pm 0.23 \ , \quad (6)$$

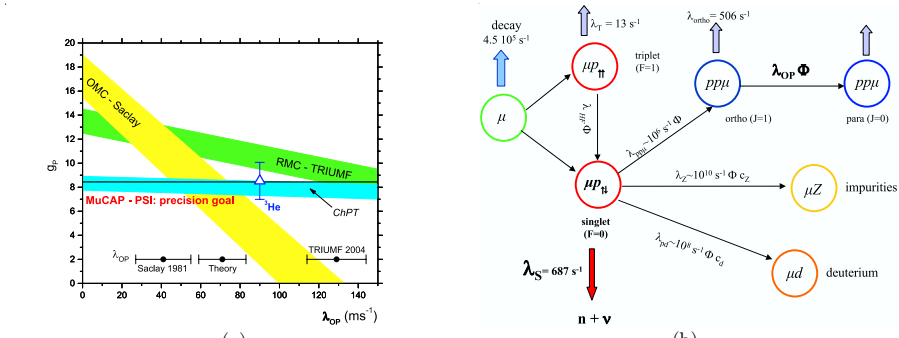

(a) (b)

Figure 4: a) Present knowledge of g_P: The OMC [10] and RMC [12] results and their λ_{OP} dependence are shown together with the error goal for MuCAP plotted at the PCAC value. The blue triangle shows the ^{3}He result [11] at an arbitrary λ_{OP} value. The line shows the calculation from Ref.[8]. The λ_{OP} values from experiments [14, 15] and theory [16] are indicated on the bottom.
b) Schematic view of important muonic processes in a hydrogen target, highlighting the capture in the μp_{1s} state and competing background processes (λ = rate, Φ = density, c = concentration).

depending on the exact values of the pion-nucleon coupling constant $g_{\pi NN}$ and the mean axial radius of the nucleon r_A. The Standard Model based calculation of the singlet muon capture rate by Govaerts and Lucio-Martinez [9] has reached 0.55% precision. This precision in calculation will allow a high precision measurement to distinguish between the pion pole contribution to g_P and the correction term. Moreover, such a measurement will also set tight limits on various theoretical scenarios beyond the Standard Model [9].

The present experimental knowledge of g_P is unsatisfying, and discrepancies cause considerable debate. Determinations via ordinary muon capture in hydrogen (OMC) [10], ^{3}He [11] and larger nuclei essentially confirm the theory result. However the precision of the latter is troubled by model dependencies. A radiative muon capture on the proton (RMC) experiment [12], which measured an additionally very rarely emitted high energy γ ray in conjunction with the muon capture process, yielded a different result[1]. The present most likely explanation lies in the insufficient knowledge of the complex kinetics of negative muons in hydrogen. The μp atom is formed in statistically populated singlet and triplet states, and the muon capture rate from these states differ by a factor of $\sim$60 due to the strong spin dependence of weak interactions. An exact knowledge of the spin populations is therefore mandatory for the interpretation of a measurement. The initial μp populations are modified via spin flip and molecular formation processes, which eventually yield a fraction of muonic hydrogen molecules ($pp\mu$). The respective rates for both

[1]While the RMC process has a 10^5 times lower branching than OMC, the emitted γ can have energies up to 100 MeV. Therefore these γ's come closer to the pion pole and the measurement is in principle four times more sensitive to g_P than OMC.

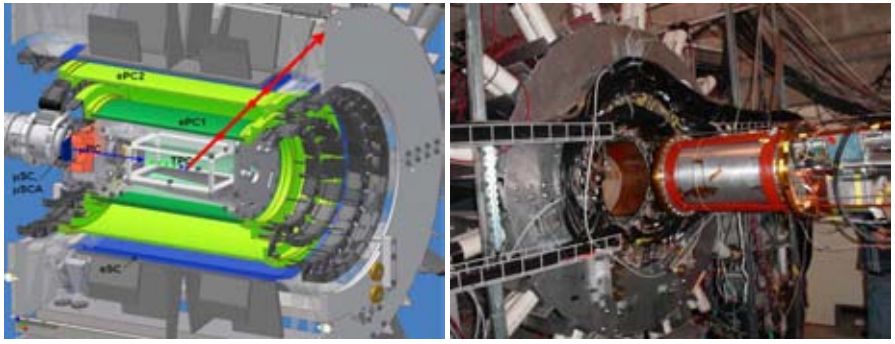

(a) (b)

Figure 5: The setup of the MuCAP experiment:
a) Schematic view of the detectors showing the muon entering from the beam channel (blue arrow), hitting the 200 μm thick time=0 scintillator (muSC) and a small wire chamber (muPC) which serves as additional pile-up counter, and then stopping in the TPC. The muon stop position is detected via a high signal caused by the Bragg peak (blue) after a track of low signals (green). The decay electron (red) is observed in 2 cylindrical wire chambers (ePC1/2) for track reconstruction. Outside is a doubled-layered scintillator hodoscope (eSC) with readout at both paddle ends, which records the decay time.
b) Installed setup in PSI's πE5 area with the hydrogen vessel rolled back, displaying the mounted μSR saddle-coil magnet.

types of process scale with density, and hence are high in the liquid hydrogen targets which were used in Refs. [10] and [12]. However, a large μ-molecular population causes a large correction to the lifetime and hence a corresponding uncertainty. Specifically the ortho to para spin-flip rate in $pp\mu$ molecules λ_{OP} (Fig.4b) is a prime suspect to cause the experimental discrepancy in g_P. Figure 4, updated from [13], shows the λ_{OP} dependence of the OMC and RMC results. The controversial λ_{OP} values are also shown. Two experimental values from Saclay [14] and TRIUMF [15], which were obtained together within the same experiments performing the OMC and RMC measurements, strongly disagree, and the only theoretical calculation [16] does not clarify the situation. It is evident that using the λ_{OP} rate from the same measurements brings the g_P value in agreement with theory. However, the use of the other λ_{OP} value enlarges the disagreement to the prediction or lowers it to an unphysical negative value. Clearly only a new determination of g_P independent of λ_{OP} can resolve this situation.

The experimental principle of the MuCAP (**Mu**on **CAP**ture) experiment is based on the measurement and comparison of the decay time of positive and negative muons in hydrogen. The MuCAP experiment is designed to overcome the multiple difficult problems of previous experiments. The important conceptual advantage of MuCAP is the selection of target hydrogen at gaseous density (10 bar at room temperature), which minimizes the kinetics dependence of the result on g_P as shown in Fig.4a. At low densities, muon

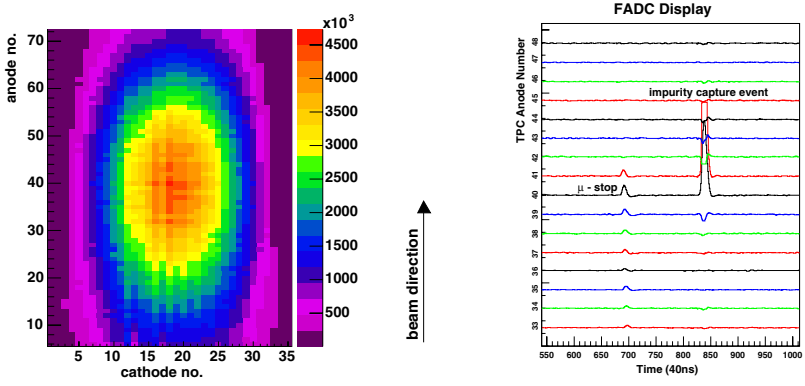

(a) (b)

Figure 6: a) Observed $2{\times}10^9$ muon stopping positions in the TPC (fall 2004).
b) Observed special event in the TPC: A muon stops after leaving a track over several anodes with a few times higher energy deposition in the last anodes. In fall 2004 we observed a fraction of $\sim 10^{-6}$ high-Z capture events, corresponding to a 10^{-8} concentration of impurities, with a clear signature of a very high signal within 25 μs after a muon stop.

capture occurs almost exclusively from the singlet state on the proton, and even a large estimated error on λ_{OP} results only in a systematic error on the 10 ppm level. The full setup is shown in Fig.5. The active gaseous hydrogen target, a time projection chamber (TPC), allows for a full 3-dimensional reconstruction of the muon path to its stopping point and therefore a selection of clean muon stops away from walls and wires. The observed stopping distribution of muons is shown in Fig.6a.

The TPC also detects muon capture events on impurity atoms ($Z > 1$) via the very large signals generated from capture products. Thus the TPC serves also as a very sensitive impurity monitor. The high rates of muon transfer to and nuclear capture on high-Z atoms (Fig.4b) can cause a deflection of the exponential lifetime even at very low impurity concentrations as these rates are typically orders of magnitude higher than muon decay. In order to minimize this effect, target purity requirements are very stringent, with the goal to be on the 10^{-9} contamination level for the sum of high-Z atoms. Additionally, the exact knowledge of these contaminations is necessary to calculate the correction factor to the lifetime. Consequently, the hydrogen gas after production in electrolysis is filled via a palladium filter and continuously run through a Zeolite based purification system (CHUPS). The CHUPS system [19] is specifically designed to maintain the hydrogen flow with negligible variations in density or hence in TPC gain. In fall 2004 we maintained clean target conditions (as low as 70 ppb impurities) for over 5 weeks.

MuCAP fully separates the muon and electron detectors to avoid dangerous cross-correlations. Decay electron times are measured in the scintillator hodoscope (eSC) sur-

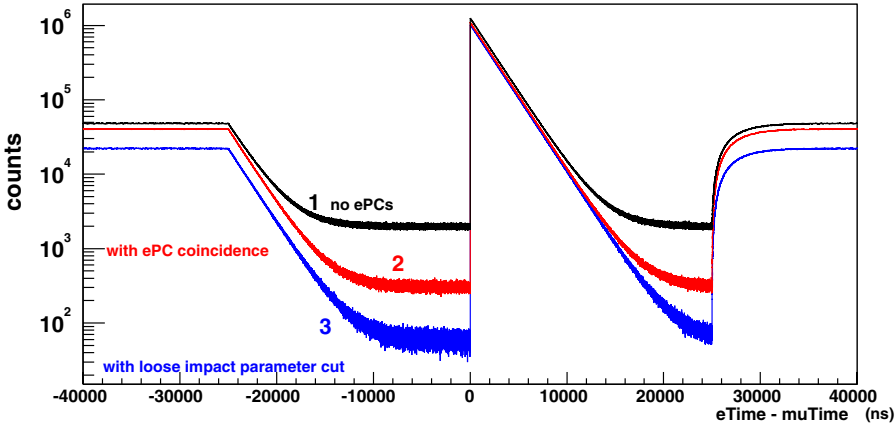

Figure 7: Preliminary muon lifetime spectrum obtained with μ^- from the MuCAP fall 2004 run. The three different curves show the benefits of the decay electron detection by the two wire chambers. Curve 1 (black) is obtained with requirement of a clean pileup-free muon stop in the TPC and a four-fold eSC coincidence hit. Curve 2 (red) requires a time coincident hit in both ePC1 and ePC2. Curve 3 (blue) additionally tracks the observed electron and requires less than 10 cm impact parameter (approximately the sensitive TPC volume). The huge reduction in background is obvious. The necessary ± 25 μs pileup veto is responsible for the background's shape.

rounding the hydrogen vessel. Two cylindrical wire chambers track the electron back in 3 dimensions to its μ-stop origin, thus largely reducing the background.

The impact parameter, defined as the minimal distance between detected muon stop and electron track, serves as an important handle on a very subtle systematic effect on the lifetime: the diffusion of muons which transfer to deuterium, an isotope always present in hydrogen. Although we are using special deuterium-depleted hydrogen, ("protium"), with deuterium content as low as 1.5 ppm, this deuterium concentration is still high enough to cause a visible effect in our setup via electron tracks with dislocated origin. This dislocation, due to μd diffusion over macroscopic distances is possible because of a Ramsauer-Townsend minimum in the $\mu d + p$ scattering cross-section at low energies. Such μd's can hit a wall or wire, transfer and then undergo unobserved nuclear capture outside the sensitive volume. The electron wire chamber tracking identifies such events and the corresponding lifetime dependence on the impact parameter will allow us to determine the deuterium contamination in situ [17]. Additionally, we have been developing a precision trace deuterium detection method via $pd\mu$ fusion [18].

As in MuLAN, MuCAP applies a magnetic field to control muon spin rotation effects

in the μ^+ measurement. A water-cooled aluminum coil was developed to minimize decay electron scattering.

Eventually MuCAP needs 10^{10} cleanly observed decay electrons and positrons to statistically reach the goal of 1 % in the capture rate, reflecting 10 ppm in the respective muon lifetimes. This is possible in several weeks of running in the fully pile-up protected mode. In the future we also intend to use the MuLAN kicked beamline with the MuCAP experiment and operate it in a "muon on request mode" [20].

Fig.7 shows a preliminary lifetime plot from our fall 2004 data. One can clearly see the huge improvement in background reduction due to the implementation of the two cylindrical wire chambers. The shown $\sim 2\times 10^9$ "clean" μ decay events are presently being analyzed, and a first result on g_P is expected in late 2005.

3 Summary

Both experiments, MuCAP and MuLan, are on the way to reach ultimate precision in their respective measurements. First physics results are expected in late 2005.

Acknowledgments I would like to express my cordial thanks to all colleagues in the MuLAN and MuCAP collaboration for creating a great scientific working environment and for their personal friendship. This work was supported by the US Department of Energy and the National Science Foundation.

References

[1] **MuCAP Collaboration:** T.I. Banks, T.A. Case, K.M. Crowe, S.J. Freedman, F.E. Gray, and B. Lauss (University of California, Berkeley and LBNL); R.M. Carey and J. Paley (Boston University); D. Chitwood, S.M. Clayton, P.T. Debevec, D.W. Hertzog, P. Kammel, B. Kiburg, R. McNabb, F. Mulhauser, C.J.G. Onderwater, C.S. Özben, and D. Webber (University of Illinois at Urbana-Champaign); T. Gorringe, M. Ojha, and P. Zolnierzcuk (University of Kentucky); L. Bonnet, J. Deutsch, J. Govaerts, D. Michotte, and R. Prieels (Université Catholique de Louvain); F.J. Hartmann (Technische Universität München); P.U. Dick, A. Dijksman, J. Egger, D. Fahrni, M. Hildebrandt, A. Hofer, L. Meier, C. Petitjean, and R. Schmidt (Paul Scherrer Institut); V.A. Andreev, B. Besymjannykh, A.A. Fetisov, V.A. Ganzha, V.I. Jatsoura, P. Kravtsov, A.G. Krivshich, E.M. Maev, O.E. Maev, G.E. Petrov, S. Sadetsky, G.N. Schapkin, G.G. Semenchuk, M. Soroka, V. Trofimov, A. Vasiliev, A.A. Vorobyov, and M. Vznuzdaev (Petersburg Nuclear Physics Institute). *http : //www.npl.uiuc.edu/exp/mucapture/*
http : //weak0.physics.berkeley.edu/weakint/research/muons/mucap_home.html

[2] **MuLAN Collaboration:** T.I. Banks, K.M. Crowe, F.E. Gray, and B. Lauss (U. of California, Berkeley and LBNL); R.M. Carey, W. Earle, A. Gafarov, B. Graf, K.R. Lynch, Y. Matus, J.P. Miller, Q. Peng, and B.L. Roberts (Boston University); D. Chitwood, S.M. Clayton, P.T. Debevec, D.W. Hertzog, P. Kammel, B. Kiburg, R. McNabb, F. Mulhauser, and D. Webber (University of Illinois at Urbana-Champaign); C.S. Özben (Istanbul Technical University); E. Bartel, C. Church, M.L. Dantuono, R. Esmaili, and K. Giovanetti

(James Madison University); S. Cheekatamalla, S. Dhamija, T. Gorringe, M. Ojha, and S. Rath (University of Kentucky). C.J.G. Onderwater (Kernfysisch Versneller Instituut, Groningen) *http* : *//www.npl.uiuc.edu/exp/mulan/*
http : *//weak0.physics.berkeley.edu/weakint/research/muons/mulan_home.html*

[3] J. Erler and M. Ramsey-Musolf, Prog. Part. Nucl. Phys. 54 (2005) 351.
[4] W. Hollik *et al.*, Acta Phys. Polon. B35 (2004) 2711.
[5] S. Eidelmann *et al.*, Phys. Lett. B592 (2004) 1.
[6] P. Kammel, Proc. of the Int. Workshop on Exotic Atoms - Future Perspectives, EXA'02, published by the Austrian Academy of Sciences Press, Vienna 2003.
[7] S. Weinberg, Phys. Rev. 112 (1958) 1375.
[8] V. Bernard, N. Kaiser, U.-G. Meissner, Phys. Rev. D 50 (1994) 6889, and V. Bernard, L. Elouadrhiri, U.-G. Meissner, J. Phys. G 28 (2002) R1.
[9] J. Govaerts and J.-L. Lucio-Martinez, Nucl. Phys. A 678 (2000) 110.
[10] G. Bardin *et al.*, Nucl. Phys. A352 (1981) 365.
[11] P. Ackerbauer *et al.*, Phys. Lett. B 417 (1998) 224.
[12] G. Jonkmans *et al.*, Phys. Rev. Lett. 77 (1996) 4512.
[13] T. Gorringe and H.W. Fearing, Rev. Mod. Phys. 76 (2004) 31.
[14] G. Bardin *et al.*, Phys. Lett. 104B (1981) 320.
[15] The TRIUMF RMC group (D. Armstrong *et al.*) has not yet released their final result on the λ_{OP} measurement. At the APS 2004 spring meeting in Denver, CO (USA), the following values have been presented, depending on the final deuterium concentration in the protium target: $\lambda_{OP} = 13.8 \pm 1.6 \times 10^{-4} s^{-1}$ (for maximum estimated D_2 contamination), and $\lambda_{OP} = 12.2 \pm 1.6 \times 10^{-4} s^{-1}$ (for no D_2 presence).
[16] D.D. Bakalov *et al.*, Nucl. Phys. A384 (1982) 302.
[17] P. Kammel. Internal MuCAP Note 29, 2003.
[18] B. Lauss, P. Kammel, A. Vasilyev, Internal MuCAP Note 30, 2005.
[19] A. Vasilyev *et al.*, Proceedings of the "NHA Annual Hydrogen Conference 2005", Washington DC, USA, March 2005.
[20] P. Kammel, Hyp. Int. 118 (1999) 323.